Bending Analysis of Two Directional Functionally Graded Beams Using A Four-Unknown Shear and Normal Deformation Theory

Araştırma Makalesi / Research Article

Armağan KARAMANLI[*]

Mühendislik ve Mimarlık Fakültesi, Mekatronik Mühendisliği Bölümü, İstanbul Gelişim Üniversitesi, Türkiye

ABSTRACT

The bending behaviour of two-directional functionally graded beams (FGBs) subjected to various sets of boundary conditions is investigated by using a shear and normal deformation theory and the Symmetric Smoothed Particle Hydrodynamics (SSPH) method. A simply supported conventional FGB problem is studied to validate the developed code. The comparison studies are performed along with the analytical solutions and the results from previous studies. The numerical calculations in terms of maximum dimensionless transverse deflections, dimensionless axial and transverse shear stresses are performed for various gradation exponents, aspect ratios (L/h) and sets of boundary conditions. The effects of the gradation exponents on the accuracy and the robustness of the SSPH method are also investigated for the two directional functionally graded beams which are having clamped-free boundary condition..

Keywords: Meshless method, Functionally graded beam, SSPH method, Shear and normal deformation theory.

Dört Bilinmeyenli Kayma ve Normal Deformasyon Teorisi Kullanılarak İki Yönlü Fonksiyonel Derecelendirilmiş Kirişlerin Eğilme Analizleri

ÖZ

Kesme ve normal deformasyon teorisi ve Simetik Düzgünleştirilmiş Parçacık Hidrodinamiği (SSPH) kullanılarak, çeşitli sınır koşullarına tabi tutulmuş iki yönlü fonksiyonel derecelendirilmiş kirişlerin (FGBs) eğilme davranışı araştırıldı. Geliştirilen kodun doğrulanması için basit mesnetlenmiş bir fonksiynel derecelendirilmiş kiriş problem üzerinde çalışıldı. Karşılaştırma çalışmaları, analitik çözümler ve daha önceki çalışmaların sonuçları vasıtasıyla gerçekleştirildi. Çeşitli üst dereceleri, en-boy oranları (L/h), ve sınır koşulları için maksimum boyutsuz çökme değerleri, boyutsuz eksenel ve kayma gerilmeleri şeklinde numerik hesaplamalar yapıldı. Ankastre-serbest uç şeklinde sınır koşullarına sahip iki yönlü fonksiyonel derecelendirilmiş kirişler için, üst derecelerinin, SSPH yönteminin doğruluğu ve gücü üzerindeki etkileri de araştırıldı.

Anahtar Kelimeler: Ağsız yöntem, Fonksiyonel derecelendirilmiş kiriş, SSPH yöntemi, Kayma ve normal deformasyon teorisi.

1. INTRODUCTION

In recent years, the use of the structures which are made of composite materials have been increasing in many modern engineering applications such as aerospace, marine, automotive, and civil engineering due to attractive properties in strength, stiffness and lightness.

Researchers have been developed various beam theories for analysis of the structural behaviour of the composite beams during the last decade, the review of these theories is given in [1]. The Euler-Bernoulli beam theory (EBT) is widely used to solve the bending behaviour of the thin beams. When the beam is thick or short, the effect of the transverse shear deformation cannot be neglected and refined shear deformation theories are needed. One of the theories which have been developed to eliminate the

assumption which is Functionally Graded Materials (FGMs) are composite materials which can be classified as advanced materials. The FGMs are inhomogeneous and made up of two (or more) different materials combined in solid states with varying properties as the dimension changes. There is a rapid increase in the use of these materials especially in the following areas; the aerospace, biomedical, defense, energy, optoelectronics, automotive, turbine blade, reactor components and etc. Since the FGMs have lower transverse shear stresses, high resistance to temperature shocks and no interface problems through the layer interfaces, they have advantages over the conventional and classical composite materials.

Due to the significant shear deformation effects especially for the thick FGBs, three main theories that are first-order shear deformation theory, higher-order shear deformation theory and shear and normal deformation

---
[*] Sorumlu Yazar (Corresponding Author)
e-posta : armagan_k@yahoo.com

theory have been employed by the researchers to predict and to understand the static, vibration and buckling responses of these structures during the last decade [1-24]. On the other hand, the conventional FGMs (or 1D-FGM) with material properties which vary in one direction used in practical engineering applications are not efficient to fulfill the technical requirements such as the temperature and stress distributions in two or three direction for aerospace craft and shuttles [25].

A new type FGM with material properties varying in two or three directions is needed to overcome this deficiency of the conventional FGM. To eliminate the drawback of the conventional FGM, the mechanical and thermal behaviours of two-directional FG structures have been investigated so far. 2D steady-state free and forced vibrations of two-directional FGBs by using the Element Free Galerkin Method are analyzed in [26]. The state-space based differential quadrature method is employed to obtain the semi-analytical elasticity solutions for bending and thermal deformations of FGBs with various end conditions [27]. A symplectic elasticity solution for static and free vibration analyses of two-directional FGBs with the material properties varying exponentially in both axial and thickness direction is presented in [28]. The buckling of Timoshenko beams composed of two directional FGM is studied in [29]. The static behavior of the two directional FGBs by using various beam theories is presented in [30]. The flexure of the two directional FG sandwich beams is analyzed in [31].

As it is seen from above discussions, the studies employing a shear and normal deformation theory which includes both shear deformation and thickness stretching effects related to static and dynamic analysis of the two-directional FGBs are very limited according to the author knowledge. Since, thickness-stretching effect becomes very important especially for the thick two directional FGBs, a shear and normal deformation theory should be considered for this complicated problem with various end conditions, aspect ratios and gradation exponents. One may easily show that the numerical methods such as finite element methods (FEM), meshless methods, GDQM, etc. can be used to overcome this problem which have complex governing equations.

Meshless methods are the most promising and have attracted considerable attention for the analysis of engineering problems with intrinsic complexity. Meshless methods are widely used in static and dynamic analyses of the isotropic, laminated composite and FGM beam problems [32-38]. However, the studies are very limited regarding to the analysis of two directional FG structures by employing a meshless method [26, 30, 39-41].

The main novelty of this paper is that the flexure behavior of the two directional FGBs is analyzed based on a quasi-3D theory by using the SSPH method with four different end conditions. Moreover, the weight (kernel) functions used for the numerical computations by employing the SSPH method given in [30, 42-45] cannot provide

satisfactory results for the solution of these complex engineering problems. To overcome this deficiency, a weight function [46] which is used for the interpolation by employing the compactly supported radial basis function is introduced. And finally, the thickness stretching effect is important and should be considered especially for the thick beams.

In section 2, the formulation of the basis function of the SSPH method is given. In section 3, the homogenization of material properties of the two directional FGB is presented. The formulation of the shear and normal deformation theory is given in Section 4. In Section 5, numerical results are given for the problems with four different boundary conditions which are simply supported (SS), clamped- simply supported (CS), clamped-clamped (CC) and clamped-free (CF).

2. FORMULATION OF SYMMETRIC SMOOTHED PARTICLE HYDRODYNAMICS METHOD

Taylor Series Expansion (TSE) of a scalar function for 1D case can be given by

$$f(\xi) = f(x) + (\xi - x)f'(x) + \frac{1}{2!}(\xi - x)^2 f''(x) +$$

$$+ \frac{1}{3!}(\xi - x)^3 f'''(x) + \frac{1}{4!}(\xi - x)^4 f^{(IV)}(x) +$$

$$\frac{1}{5!}(\xi - x)^5 f^{(V)}(x) + \frac{1}{6!}(\xi - x)^6 f^{(VI)}(x) + \dots \quad (1)$$

where $f(\xi)$ is the value of the function at ξ located in near of x. If the seventh and higher order terms are neglected, the Eq. (1) can be expressed as

$$f(\xi) = \boldsymbol{P}(\xi, x)\boldsymbol{Q}(x) \quad (2)$$

where

$$\boldsymbol{Q}(x) = \left[f(x), \frac{df(x)}{dx}, \frac{1}{2!}\frac{d^2 f(x)}{dx^2}, \dots, \frac{1}{6!}\frac{d^6 f(x)}{dx^6} \right]^T \quad (3)$$

$$\boldsymbol{P}(\xi, x) = [1, (\xi - x), (\xi - x)^2, \dots, (\xi - x)^6] \quad (4)$$

The order of the governing equations play an important role to define the number of terms assigned in the Taylor series expansion. If the number of terms in the TSE is increased, there will be an increment in the CPU time and one may expect that the accuracy will increase. However, in some cases it may not be true and determination of the number of terms depends on the researcher's experience. To determine the unknown variables given in the $\boldsymbol{Q}(x)$, both sides of Eq. (2) are multiplied with $W(\xi, x)\boldsymbol{P}(\xi, x)^T$ and evaluated for every node in the CSD. In the global numbering system, let the particle number of the jth particle in the compact support of $W(\xi, x)$ be r (j). The following equation is obtained

$$\sum_{j=1}^{N(x)} f(\xi^{r(j)}) W(\xi^{r(j)}, x) \boldsymbol{P}(\xi^{r(j)}, x)^T$$

$$= \sum_{j=1}^{N(x)} \left[\boldsymbol{P}(\xi^{r(j)}, x)^T W(\xi^{r(j)}, x) \boldsymbol{P}(\xi^{r(j)}, x) \right] \boldsymbol{Q}(x) \quad (5)$$

where N(x) is the number nodes in the compact support domain (CSD) of the $W(\xi, x)$ as shown in Figure 1.
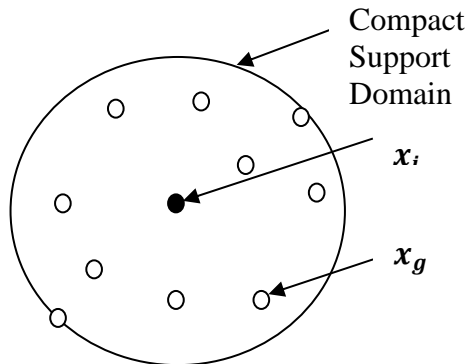
Then, Eq. (5) can be given by

$$C(\xi,x)Q(x) = D(\xi,x)F^{(x)}(\xi,x) \tag{6}$$

Where $C(\xi,x) = P(\xi,x)^T W(\xi,x)P(\xi,x)$ and $D(\xi,x) = P(\xi,x)^T W(\xi,x)$.

The solution of Eq. (6) is given by

$$Q(x) = K(\xi,x)F(\xi) \tag{7}$$

where $K^{(x)}(\xi,x) = C(\xi,x)^{-1}D(\xi,x)$.

Figure 1. Compact support of the weight function $W(\xi,x)$ for the node located at $x = (x_i, y_i)$.

Eq. (7) can be also written as follows

$$Q_I(x) = \sum_{J=1}^{M} K_{IJ}F_J \ , \qquad I = 1,2,\dots,7 \tag{8}$$

where M is the number of nodes and $F_J = f(\xi^J)$. Seven components of Eq. (8) for 1D case are written as

$$f(x) = Q_1(x) = \sum_{J=1}^{M} K_{1J}F_J$$

$$\frac{df(x)}{dx} = Q_2(x) = \sum_{J=1}^{M} K_{2J}F_J$$

$$\frac{d^2f(x)}{dx^2} = 2! \, Q_3(x) = 2! \sum_{J=1}^{M} K_{3J}F_J$$

$$\frac{d^3f(x)}{dx^3} = 3! \, Q_4(x) = 3! \sum_{J=1}^{M} K_{4J}F_J$$

$$\frac{d^4f(x)}{dx^4} = 4! \, Q_5(x) = 4! \sum_{J=1}^{M} K_{5J}F_J$$

$$\frac{d^5f(x)}{dx^5} = 5! \, Q_6(x) = 5! \sum_{J=1}^{M} K_{6J}F_J$$

$$\frac{d^6f(x)}{dx^6} = 6! \, Q_7(x) = 6! \sum_{J=1}^{M} K_{7J}F_J \tag{9}$$

Details of the SSPH method can be found in [30, 42-45].

3. HOMOGENIZATION OF MATERIAL PROPERTIES

We assume that the two-directional functionally graded beam of length L, width b, thickness h is made of two different constituents. Further, the material properties vary not only in the z direction (thickness direction) but also in the x direction (along the length of the beam) as shown in Fig. 2. The rule of mixture is used to find the effective material properties at a point. According to the rule of mixtures, the effective material properties of the beam, Young's modulus E and shear modulus G can be given by In Figure 2.
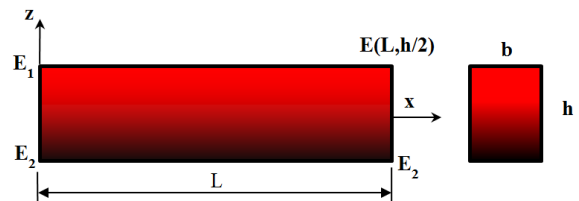
Figure 2. Geometry and coordinate of a two-directional FGB.

The stress-strain relationship of a kth orthotropic lamina in the material coordinate axes is given by:

$$E(x,z) = E_1 V_1(x,z) + E_2 V_2(x,z)$$

$$G(x,z) = G_1 V_1(x,z) + G_2 V_2(x,z) \tag{10}$$

where E_1, E_2, G_1 and G_2 are the material properties of two constituents, V_1 and V_2 are volume fractions of the constituents. The relation of the volume fractions can be expressed as follows;

$$V_1(x,z) + V_2(x,z) = 1 \tag{11}$$

According to the power law form, the volume fraction of the constitute 1 can be given

$$V_1(x,z) = \left(1 - \frac{x}{2L}\right)^{p_x} \left(\frac{1}{2} + \frac{z}{h}\right)^{p_z} \tag{12}$$

where p_x and p_z are the gradation exponents (power-law index) which determine the material properties through the thickness (h) and length of the beam (L), respectively. When the p_x and p_z are set to zero then the beam becomes homogeneous. The effective material properties can be found by using the Eqs. (10), (11) and (12) as follows

$$E(x,z) = (E_1 - E_2)\left(1 - \frac{x}{2L}\right)^{p_x}\left(\frac{1}{2} + \frac{z}{h}\right)^{p_z} + E_2$$

$$G(x,z) = (G_1 - G_2)\left(1 - \frac{x}{2L}\right)^{p_x}\left(\frac{1}{2} + \frac{z}{h}\right)^{p_z} + G_2 \tag{13}$$

Fig.3 illustrates the variation of the dimensionless modulus of elasticity through the depth of the beam for various values of the gradation exponent (p_z) in the z direction. The variation of the dimensionless modulus of elasticity through the length of the beam for different gradation exponent (p_x) in the x direction is presented in Fig. 4.
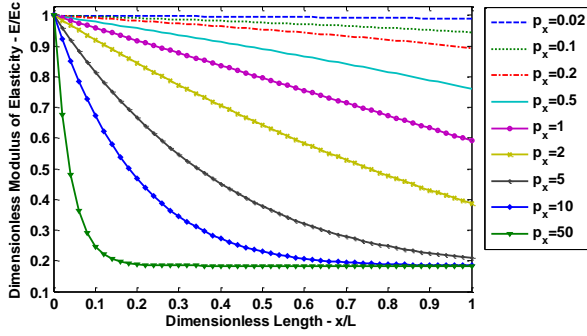
Figure 3. Variation of the dimensionless modulus of elasticity through the depth of the beam for various values of the gradation exponent (p_z) in z direction
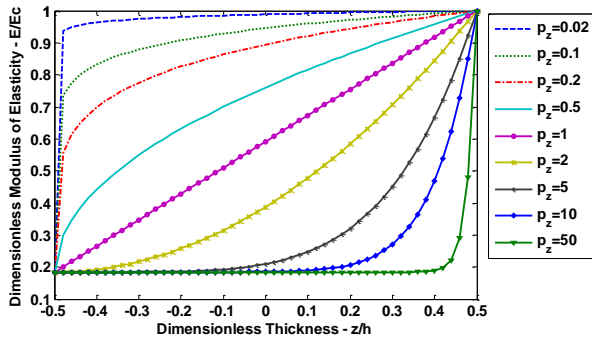
Figure 4. Variation of the dimensionless modulus of elasticity through the length of the beam for different gradation exponent (p_x) in x direction

4. MATHEMATICAL FORMULATION

The axial and transverse displacements of a beam by using the present shear and normal deformation theory [17] including both shear deformation and thickness stretching effects are given by

$$U(x,z) = u(x,t) - z\frac{dw_b(x)}{dx} - \frac{4z^3}{3h^2}\frac{dw_s(x)}{dx}$$
$$= u(x) - zw_b'(x) - f(z)w_s'(x) \quad (14a)$$

$$W(x,z) = w_b(x) + w_s(x) + \left(1 - \frac{4z^2}{h^2}\right)w_z(x)$$
$$= w_b(x) + w_s(x) + g(z)w_z(x) \quad (14b)$$

where u, w_b, w_s and w_z are four variables to be determined.

The only nonzero strains associated with the displacement field given in Eq. (14) can be written by:

$$\varepsilon_x = \frac{\partial U}{\partial x} = u' - zw_b'' - f(z)w_s'' \quad (15a)$$

$$\varepsilon_z = \frac{\partial W}{\partial z} = g'(z)w_z \quad (15b)$$

$$\gamma_{xz} = \frac{\partial W}{\partial x} + \frac{\partial U}{\partial z} = g(z)(w_s' + w_z') \quad (15c)$$

The following linear elastic constitutive equation can be written by using the related stresses and strains:

$$\begin{bmatrix} \sigma_x \\ \sigma_z \\ \sigma_{xz} \end{bmatrix} = \frac{E(x,z)}{1-v^2}\begin{bmatrix} 1 & v & 0 \\ v & 1 & 0 \\ 0 & 0 & \frac{1-v}{2} \end{bmatrix}\begin{bmatrix} \varepsilon_x \\ \varepsilon_z \\ \gamma_{xz} \end{bmatrix} \quad (16)$$

To obtain the governing equations, the virtual strain energy of the beam can be written as:

$$\delta U = \int_0^L \int_A (\sigma_x \delta\varepsilon_x + \sigma_{xz}\delta\gamma_{xz} + \sigma_z g'\delta\varepsilon_z)dAdx \quad (17)$$

The stress resultants $N_x, M_x^b, M_x^s, Q_{xz}$ and R_z can be written respectively as follows:

$$N_x = \int_{-h/2}^{+h/2} b\sigma_x dz \quad (18a)$$

$$M_x^b = \int_{-h/2}^{+h/2} b\sigma_x z dz \quad (18b)$$

$$M_x^s = \int_{-h/2}^{+h/2} b\sigma_x f dz \quad (18c)$$

$$Q_{xz} = \int_{-h/2}^{+h/2} b\sigma_{xz} g dz \quad (18d)$$

$$R_z = \int_{-h/2}^{+h/2} b\sigma_z g' dz \quad (18e)$$

Using the Eq. (18), one can rewrite the Eq. (17) as:

$$\delta U = \int_0^L [N_x\delta u' - M_x^b\delta w_b'' - M_x^s\delta w_s'' + Q_{xz}(\delta w_s' + \delta w_z') + R_z\delta w_z]dx \quad (19a)$$

The virtual potential energy of the transverse load $q(x)$ is given by

$$\delta V = -\int_0^L q(\delta w_b + \delta w_s)dx \quad (20)$$

Since the total virtual work done equals zero and the coefficients of $\delta u, \delta w_b, \delta w_s$ and δw_z are zero in $0 < x < L$, one can obtain the following governing equations,

$$\frac{dN_x}{dx} = 0 \quad (21a)$$

$$\frac{d^2M_x^b}{dx^2} + q(x) = 0 \quad (21b)$$

$$\frac{d^2M_x^s}{dx^2} + \frac{dQ_{xz}}{dx} + q(x) = 0 \quad (21c)$$

$$\frac{dQ_{xz}}{dx} - R_z = 0 \quad (21d)$$

Using Eq. (16), the stress resultants given in Eq. (18) can be expressed as,

$$\begin{Bmatrix} N_x \\ M_x^b \\ M_x^s \\ Q_{xz} \\ R_z \end{Bmatrix} = \begin{bmatrix} A & B & B_s & X & 0 \\ B & D & D_s & Y & 0 \\ B_s & D_s & H & Y_s & 0 \\ X & Y & Y_s & Z & 0 \\ 0 & 0 & 0 & 0 & A_s \end{bmatrix}\begin{Bmatrix} u' \\ -w_b'' \\ -w_s'' \\ w_z \\ w_s' + w_z' \end{Bmatrix} \quad (22)$$

where

$$(A, B, B_s, D, D_s, H, Z) =$$
$$\int_{-h/2}^{+h/2} \frac{E(x,z)b}{1-v^2}(1, z, f, z^2, fz, f^2, g'^2)dz \quad (23a)$$

$$A_s = \int_{-h/2}^{+h/2} \frac{E(x,z)b}{2(1+v)} g^2 dz \quad (23b)$$

$$(X, Y, Y_s) = \int_{-h/2}^{+h/2} \frac{E(x,z)vb}{1-v^2} g'(1, z, f)dz \quad (23c)$$

The governing equations of the quasi-3D theory can be obtained by substituting Eq. (22) into Eq. (21) as:

$$Au'' + A'u' - (Bw_b''' + B'w_b'') - (B_sw_s''' + B_s'w_s'') + Xw_z' + X'w_z = 0 \quad (24a)$$

$$Bu''' + 2B'u'' + B''u' - (Dw_b^{(IV)} + 2D'w_b''' + D''w_b'') - (D_sw_s^{(IV)} + 2D_s'w_s''' + D_s''w_s'') + Yw_z'' + 2Y'w_z' + Y''w_z - q = 0 \quad (24b)$$

$B_s u''' + 2B_s' u'' + B_s'' u' - \left(D_s w_b^{(IV)} + 2D_s' w_b''' + D_s'' w_b''\right) - \left(H w_s^{(IV)} + 2H' w_s''' + H'' w_s''\right) + Y_s w_z'' + 2Y_s' w_z' + Y_s'' w_z + A_s(w_s'' + w_z'') + A_s'(w_s' + w_z') - q = 0$ (24c)

$-Xu' + Y w_b'' + Y_s w_s'' + A_s(w_s'' + w_z'') + A_s'(w_s' + w_z') - Z w_z = 0$ (24d)

The natural boundary conditions are given as follows:

$\delta u: N_x$ (25a)

$\delta w_b: M_x^{b'}$ (25b)

$\delta w_b' : M_x^b$ (25c)

$\delta w_s: M_x^{s'} + Q_{xz}$ (25d)

$\delta w_s' : M_x^s$ (25e)

$\delta w_z: Q_{xz}$ (25f)

5. NUMERICAL RESULTS

The static behaviour of the two directional FGBs is investigated by using a quasi-3D shear deformation theory. The numerical results are obtained by using the SSPH method for various gradation exponents in both direction, x and z respectively, different aspect ratios and boundary conditions. Since there is no available previous results based on a higher order shear deformation theory and a shear and normal deformation theory for the bending analysis of two-directional FGBs with power law rule, as the first, the developed code is verified by solving a simply supported conventional FGB problem subjected to uniformly distributed load. The numerical solutions are compared with the solutions from previous studies [16-17] along with the analytical solutions. The dimensionless maximum transverse deflections, axial and shear stresses are calculated to make the comparisons on a fair ground. For each problem studied here, the physical parameters of the beam are L=2m and b=0.1m. Two different two aspect ratios (L/h), 5 and 20 are considered for the boundary conditions defined as SS, CS and CC. The numerical solutions could not be obtained for the aspect ratio (L/h) which is greater than 5 for the boundary condition defined as CF. The possible reasons behind this case are discussed in section 5.2.4. The distributed load q_0 is set to 10000 N/m. The material properties of the two constitutes are given

$Ceramic\ (Al_2O_3) \quad : E_1 = 380 GPa\ and\ \nu_1 = 0.3$

$Metal\ (Aluminium) : E_2 = 70 GPa\ and\ \nu_2 = 0.3$

The following non-dimensional quantities are used for the representation of the results;

Non-dimensional maximum transverse deflection of the beam:

$\bar{w} = \frac{100 E_2 b h^3}{q_0 L^4} W(x, 0)\ for\ SS, CS\ and\ CC\ beams \quad \bar{w} = \frac{100 E_2 b h^3}{q_0 L^4} W(L, 0)\ for\ CF\ beam$ (26)

Non-dimensional axial and shear stresses of the beam:

$\bar{\sigma}_x = \frac{bh}{q_0 L} \sigma_x(\frac{L}{2}, z)$

$\bar{\sigma}_z = \frac{bh}{q_0 L} \sigma_z(\frac{L}{2}, z)$

$\bar{\sigma}_{xz} = \frac{bh}{q_0 L} \sigma_{xz}(0, z)$ (27)

5.1 Verification and Comparison Studies

To verify the developed code, a simply supported FGB under uniformly distributed load is considered. For numerical calculations to be performed by the SSPH method uniformly distributed 201 nodes for the SS, CS and CC beams and 247 nodes for the CF beam are used in the problem domain $x \in [0, 2]$. As a weight function, the following function proposed in [46] is used,

$W(x, \xi) = \begin{cases} \left(1 - \frac{d}{\rho}\right)^7 35\left(\frac{d}{\rho}\right)^6 + 245\left(\frac{d}{\rho}\right)^5 + 720\left(\frac{d}{\rho}\right)^4 + \\ 0 \\ 1120\left(\frac{d}{\rho}\right)^3 + 928\left(\frac{d}{\rho}\right)^2 + 336\left(\frac{d}{\rho}\right) + 48 \quad 0 \le d \le \rho \\ 0 \hspace{5cm} d > \rho \end{cases}$ (28)

where $d = |x - \xi|/h$, h is the smoothing length and ρ is the scaling factor that determines the size of the support domain. The numerical calculations are performed according to the following meshless parameters; the radius of the support domain (ρ) is chosen as 8 and the smoothing length (h) equals to 1.1Δ where Δ is the minimum distance between two adjacent nodes for SS, CS and CC beams. For CF beam, the radius of the support domain (ρ) is chosen as 5.302 and the smoothing length (h) equals to 1.2Δ. All the meshless parameters are found by using the trial and error method. The maximum non-dimensional transverse deflections, axial, normal and shear stresses obtained based on the present shear and normal deformation theory, various aspect ratios and various gradation exponents in the z direction are given in Table 1-4 along with the results from previous studies and the analytical solution of the problem. It is clear that the results obtained by using the SSPH method agree completely with those of previous papers [16-17]. Table 1-4 show that the results obtained by the SSPH method are in excellent agreement with the results given in [16-17]. And finally, because of stretching effect, the transverse deflections computed based on the shear and normal deformation theory are slightly smaller than those obtained from TBT. Due to this agreement, the verification of the developed code is established.

Table 1. Verification studies of the developed meshless code for SS FGB, dimensionless maximum transverse deflections for various gradation exponents.

Method	Theory	ε_z	p = 0	p = 1	p = 2	p = 5	p = 10
L/h=5							
Li et al. [16]	TBT	= 0	3.1657	6.2599	8.0602	9.7802	10.8979
Vo et al. [17] Navier	TBT	= 0	3.1654	6.2594	8.0677	9.8281	10.9381
	Present	≠ 0	3.1397	6.1338	7.8606	9.6037	10.7578
Vo et al. [17] FEM	TBT	= 0	3.1654	6.2590	8.0668	9.8271	10.9375
	Present	≠ 0	3.1397	6.1334	7.8598	9.6030	10.7572
SSPH	Present	≠ 0	3.1402	6.1343	7.8602	9.6041	10.7571
L/h=20							
Li et al. [16]	TBT	= 0	2.8962	5.8049	7.4415	8.8151	9.6879
Vo et al. [17] Navier	TBT	= 0	2.8962	5.8049	7.4421	8.8182	9.6905
	Present	≠ 0	2.8947	5.7201	7.2805	8.6479	9.5749
Vo et al. [17] FEM	TBT	= 0	2.8963	5.8045	7.4412	8.8173	9.6899
	Present	≠ 0	2.8947	5.7197	7.2797	8.6471	9.5743
SSPH	Present	≠ 0	2.8952	5.7215	7.2826	8.6485	9.5745

Table 2. Verification studies of the developed meshless code for SS FGB, dimensionless axial stress $\bar{\sigma}_x(\frac{L}{2},\frac{h}{2})$ for various gradation exponents.

Method	Theory	ε_z	p = 0	p = 1	p = 2	p = 5	p = 10
L/h=5							
Li et al. [16]	TBT	= 0	3.8020	5.8837	6.8812	8.1030	9.7063
Vo et al. [17] Navier	TBT	= 0	3.8020	5.8836	6.8826	8.1106	9.7122
	Present	≠ 0	3.8005	5.8812	6.8818	8.1140	9.7164
Vo et al. [17] FEM	TBT	= 0	3.8040	5.8870	6.8860	8.1150	9.7170
	Present	≠ 0	3.8020	5.8840	6.8860	8.1190	9.7220
SSPH	Present	≠ 0	3.8005	5.8815	6.8821	8.1145	9.7170
L/h=20							
Li et al. [16]	TBT	= 0	15.0130	23.2054	27.0989	31.8112	38.1372
Vo et al. [17] Navier	TBT	= 0	15.0129	23.2053	27.0991	31.8130	38.1385
	Present	≠ 0	15.0125	23.2046	27.0988	31.8137	38.1395
Vo et al. [17] FEM	TBT	= 0	15.0200	23.2200	27.1100	31.8300	38.1600
	Present	≠ 0	15.0200	23.2200	27.1100	31.8300	38.1600
SSPH	Present	≠ 0	15.0147	23.2099	27.1122	31.8070	38.1252

Table 3. Verification studies of the developed meshless code for SS FGB, dimensionless transverse shear stress $\bar{\sigma}_{xz}(0,0)$ for various gradation exponents.

Method	Theory	ε_z	p = 0	p = 1	p = 2	p = 5	p = 10
L/h=5							
Li et al. [16]	TBT	= 0	0.7500	0.7500	0.6787	0.5790	0.6436
Vo et al. [17] Navier	TBT	= 0	0.7332	0.7332	0.6706	0.5905	0.6467
	Present	≠ 0	0.7233	0.7233	0.6622	0.5840	0.6396
Vo et al. [17] FEM	TBT	= 0	0.7335	0.7335	0.6700	0.5907	0.6477
	Present	≠ 0	0.7291	0.7291	0.6661	0.5873	0.6439
SSPH	Present	≠ 0	0.7246	0.7234	0.6618	0.5840	0.6396
L/h=20							
Li et al. [16]	TBT	= 0	0.7500	0.7500	0.6787	0.5790	0.6436
Vo et al. [17] Navier	TBT	= 0	0.7451	0.7451	0.6824	0.6023	0.6596
	Present	≠ 0	0.7432	0.7432	0.6809	0.6010	0.6583
Vo et al. [17] FEM	TBT	= 0	0.7470	0.7470	0.6777	0.6039	0.6682
	Present	≠ 0	0.7466	0.7466	0.6776	0.6036	0.6675
SSPH	Present	≠ 0	0.7425	0.7432	0.6789	0.6037	0.6606

Table 4. Verification studies of the developed meshless code for SS FGB, dimensionless normal stress $\bar{\sigma}_z\left(\frac{L}{2},\frac{h}{2}\right)$ for various gradation exponents.

Method	Theory	ε_z	p = 0	p = 1	p = 2	p = 5	p = 10
L/h=5							
Vo et al. [17] Navier	Present	$\neq 0$	0.1352	0.0670	0.0925	0.0180	-0.0181
Vo et al. [17] FEM	Present	$\neq 0$	0.1352	0.0672	0.0927	0.0183	-0.0179
SSPH	Present	$\neq 0$	0.1352	0.0671	0.0925	0.0182	-0.0180
L/h=20							
Vo et al. [17] Navier	Present	$\neq 0$	0.0337	-0.5880	-0.6269	-1.1698	-1.5572
Vo et al. [17] FEM	Present	$\neq 0$	0.0338	-0.5874	-0.6261	-1.1690	-1.5560
SSPH	Present	$\neq 0$	0.0338	-0.5880	-0.6266	-1.1706	-1.5589

Table 5. Boundary conditions used for the numerical computations.

BC	x=0	x=L
SS	$u = 0, w_b = 0, w_s = 0, w_z = 0, M_x^b = 0, M_x^s = 0$	$u = 0 \ or \ N_x = 0 , w_b = 0, w_s = 0, w_z = 0, M_x^b = 0, M_x^s = 0$
CS	$u = 0, w_b = 0, w_s = 0, w_z = 0, w_b' = 0, w_s' = 0$	$u = 0 \ or \ N_x = 0 , w_b = 0, w_s = 0, w_z = 0, M_x^b = 0, M_x^s = 0$
CC	$u = 0, w_b = 0, w_s = 0, w_z = 0, w_b' = 0, w_s' = 0$	$u = 0, w_b = 0, w_s = 0, w_z = 0, w_b' = 0, w_s' = 0$
CF	$u = 0, w_b = 0, w_s = 0, w_z = 0, w_b' = 0, w_s' = 0$	$N_x = 0, M_x^b = 0, M_x^s = 0, M_x^{b'} = 0, M_x^{s'} + Q_{xz} = 0, Q_{xz} = 0$

Table 6. Dimensionless maximum transverse deflections of the SS two-directional FGB for various gradation exponents in both directions and aspect ratios.

Aspect Ratio (L/h)	p_z	p_x				
		0	1	2	5	10
5	0	3.1402	3.9791	4.9566	8.2264	12.2258
	1	6.1343	7.2342	8.3430	11.2590	14.0759
	2	7.8602	8.8636	9.8333	12.3067	14.6466
	5	9.6041	10.4721	11.3126	13.4239	15.3073
	10	10.7571	11.6165	12.4207	14.2924	15.8037
20	0	2.8952	3.6662	4.5679	7.6257	11.4111
	1	5.7215	6.7299	7.7469	10.4640	13.1101
	2	7.2826	8.1853	9.0653	11.3622	13.5589
	5	8.6485	9.4397	10.2153	12.2531	14.0626
	10	9.5745	10.3974	11.1716	12.9851	14.4938

Table 7. Dimensionless axial stress $\bar{\sigma}_x(\frac{L}{2},\frac{h}{2})$ of the SS two-directional FGB for various gradation exponents in both directions.

Aspect Ratio (L/h)	p_z	p_x				
		0	1	2	5	10
5	0	3.8005	3.7945	3.7703	3.6740	3.6146
	1	5.8815	5.6196	5.3454	4.6207	3.9726
	2	6.8821	6.4155	5.9789	4.9475	4.0813
	5	8.1145	7.4802	6.8933	5.4784	4.2515
	10	9.7170	8.8501	8.0301	6.0444	4.4015
20	0	15.0147	14.9895	14.8909	14.5014	14.2517
	1	23.2099	22.1731	21.0861	18.2136	15.6904
	2	27.1122	25.2728	23.5505	19.4770	16.1494
	5	31.8070	29.3394	27.0385	21.5344	16.7800
	10	38.1252	34.7636	31.5736	23.9702	17.3768

5.2 Elastostatic Analysis of Two-Directional FGBs

Four different boundary conditions, SS, CS, CC and CF are considered respectively for the bending analysis of two directional FGBs subjected to uniformly distributed load. The transverse deflections, axial, normal and shear stresses are computed based on the present quasi-3D theory for different gradation exponents in both directions and aspect ratios. The details of the boundary conditions (BCs) used for the numerical analysis are given in Table 5.

5.2.1 SS Two-Directional FGB

A simply supported two directional FGB under uniformly distributed load is analyzed. The dimensionless transverse deflections and stresses are computed for various gradation exponents in both directions and different aspect ratios.

As it is seen from Table 6, the computed transverse deflection value decreases as the aspect ratio increases. With the increasing of the gradation exponents in both directions, the deflection values are increasing. In Table 7, the dimensionless axial stress values are presented. It is clear that the stress decreases as the gradation exponents in both directions increases. The maximum dimensionless shear stress value is obtained when p_z is set to zero and p_x is set to 5 as shown in Table 8. It is found in Table 9 that the dimensionless normal stress almost vanishes when the aspect ratio is 20 and the gradation exponent in the z direction is set to zero.

Figs. 5 and 6 are plotted for different aspect ratios to show the variation of the dimensionless axial and normal stresses through the thickness for different values of the gradation exponent in the x direction, when the gradation exponent in the z direction is determined as 2. The maximum axial stress value is observed at the top surface of the beam. The axial stress increases as the gradation exponent in the x direction decreases. The beam with $p_z=2$ and $p_x=0$ yields the maximum normal stress as seen in Figs. 5 and 6. In Figs. 5 and 6, it is also clear that the computed shear stress values are zero on the top and the bottom surfaces of the beam, as it is expected. The minimum shear stress value is obtained when the p_z is set to 10.

5.2.2 CS Two-Directional FGB

The dimensionless maximum transverse deflections and the axial, normal and shear stresses of the clamped-simply supported FGBs are investigated. The computed results are given in Table 10 and Figs. 7-8. It is clear in Table 10 that the transverse deflections increase as the gradation exponent increases. Lower aspect ratio has the larger dimensionless transverse deflections than the higher one.

In Figs. 7-8, the axial, normal and shear stresses are presented for various gradation exponents and aspect ratios. It is found that the maximum axial stress increases as the gradation exponent in the x direction increases.

The maximum normal stress is obtained at the bottom surface of the beam. The normal stress values are decreasing as the gradation exponent in the x direction is decreasing at the bottom surface of the beam. The maximum shear stress is observed for $p_z=1$ when the p_x is set to 2.

5.2.3 CC Two-Directional FGB

The dimensionless maximum transverse deflections and the axial, normal and shear stresses of the clamped-clamped FGBs are considered. The results are given in Table 11 and Fig. 9 for different gradation exponents and aspect ratios. It is clear from Table 11 that, as the gradation exponents increase, the transverse deflections increase. The computed results are in very well agreement along with the previous study.

The axial and normal stresses are plotted in Fig.9 for various gradation exponents in the x direction as the aspect ratio is set 5 and pz=0. As the gradation exponent set to zero in the z direction, the maximum axial stresses obtained for px=0 and px=1 are almost indistinguishable. The maximum normal stress values are seen on the top surface of the beam and they are also indistinguishable. The maximum normal stress is found for px=10. As it is expected, the shear stress values are zero at the bottom and top surface of the beam. The maximum shear stress is observed for pz=1.

5.2.4 CF Two-Directional FGB

Finally, the results of elastostatic analysis of the CF FGBs under uniformly distributed load are given for various gradation exponents and aspect ratios. For this example, accurate and agreed results cannot be obtained when the aspect ratio is greater than 5 and the gradation exponent is x direction greater than 2. However, the results found by using the aspect ratio lower than 6 are acceptable and agreed along with the analytical solutions. This point is important to determine future studies based on the present shear and normal shear deformation theory and the SSPH method. It is not clear that increasing the gradation exponent in the x direction deteriorates the accuracy of the present shear and normal deformation theory with higher aspect ratios. The robustness and accuracy of the SSPH method could be lost by using the gradation exponent in the x direction greater than 5 with CF boundary conditions as well.

As it is seen from Table 12, the transverse deflections increase as the gradation exponents increase. Three different aspect ratios are employed to investigate the inefficiency of the theory and the numerical method. It is not found a concrete reason that may explain the loss of accuracy when the aspect ratio is set to above 5. However, the computed results agree very well along with the analytical solutions based on the TBT.
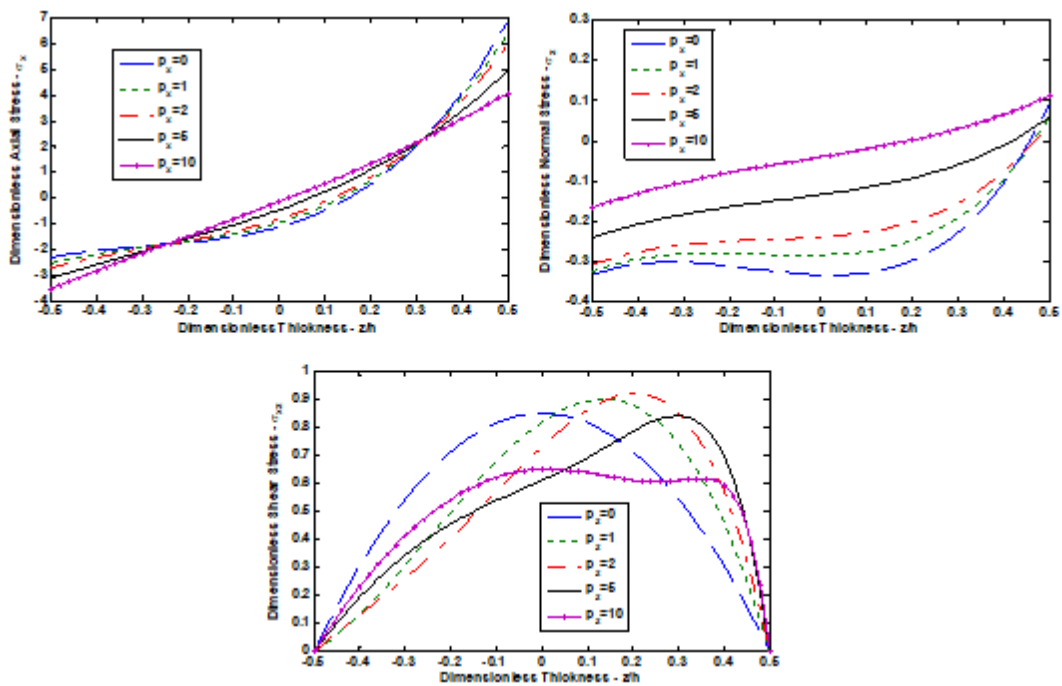
Table 8. Dimensionless transverse shear stress $\bar{\sigma}_{xz}(0,0)$ of the SS two-directional FGB for various gradation exponents in both directions.

Aspect Ratio (L/h)	p_z	p_x				
		0	1	2	5	10
5	0	0.7246	0.7923	0.8484	0.9278	0.9195
	1	0.7234	0.7780	0.8186	0.8662	0.8560
	2	0.6618	0.7017	0.7290	0.7582	0.7523
	5	0.5840	0.6001	0.6099	0.6203	0.6200
	10	0.6396	0.6457	0.6494	0.6542	0.6557
20	0	0.7425	0.8125	0.8718	0.9580	0.9467
	1	0.7432	0.7993	0.8415	0.8901	0.8778
	2	0.6789	0.7199	0.7486	0.7792	0.7740
	5	0.6037	0.6223	0.6364	0.6385	0.6414
	10	0.6606	0.6686	0.6749	0.6738	0.6791

Table 9. Dimensionless normal stress $\bar{\sigma}_z \left(\frac{L}{2}, \frac{h}{2} \right)$ of the SS two-directional FGB for various gradation exponents in both directions.

| Aspect Ratio (L/h)	p_z	p_x				
		0	1	2	5	10
5	0	0.1352	0.1350	0.1346	0.1331	0.1328
	1	0.0671	0.0553	0.0498	0.0636	0.1085
	2	0.0925	0.0583	0.0422	0.0577	0.1110
	5	0.0182	0.0108	0.0205	0.0772	0.1253
	10	-0.0180	0.0157	0.0498	0.1176	0.1396
20	0	0.0338	0.0338	0.0337	0.0333	0.0331
	1	-0.5880	-0.6015	-0.5864	-0.4229	-0.1163
	2	-0.6266	-0.7108	-0.7197	-0.5044	-0.1138
	5	-1.1706	-1.1012	-0.9656	-0.5067	-0.0843
	10	-1.5589	-1.2682	-0.9862	-0.3459	-0.0493

Figure 5. Dimensionless axial $\bar{\sigma}_x(\frac{L}{2}, z)$, normal $\bar{\sigma}_z(\frac{L}{2}, z)$ and shear stress $\bar{\sigma}_{xz}(0, z)$ through the thickness of the SS FGB for p_z=2 and p_x=2, L/h=5

Table 10. Dimensionless maximum transverse deflections of the CS two-directional FGB for various gradation exponents in both directions.

Aspect Ratio (L/h)	p_z	p_x				
		0	1	2	5	10
5	0	1.4497	1.7984	2.1844	3.3256	4.4754
	1	2.7943	3.2536	3.7003	4.7672	5.6600
	2	3.6053	4.0375	4.4382	5.3676	6.1134
	5	4.5443	4.9024	5.2356	5.9811	6.5451
	10	5.1527	5.4762	5.7665	6.3852	6.8235
20	0	1.2572	1.5297	1.8335	2.7508	3.6922
	1	2.2574	2.6612	3.0403	3.8831	4.7242
	2	2.8623	3.2657	3.6266	4.3313	4.9949
	5	3.2451	3.6310	3.8925	4.5933	5.2977
	10	3.8213	4.1552	4.3400	4,9688	5.6261
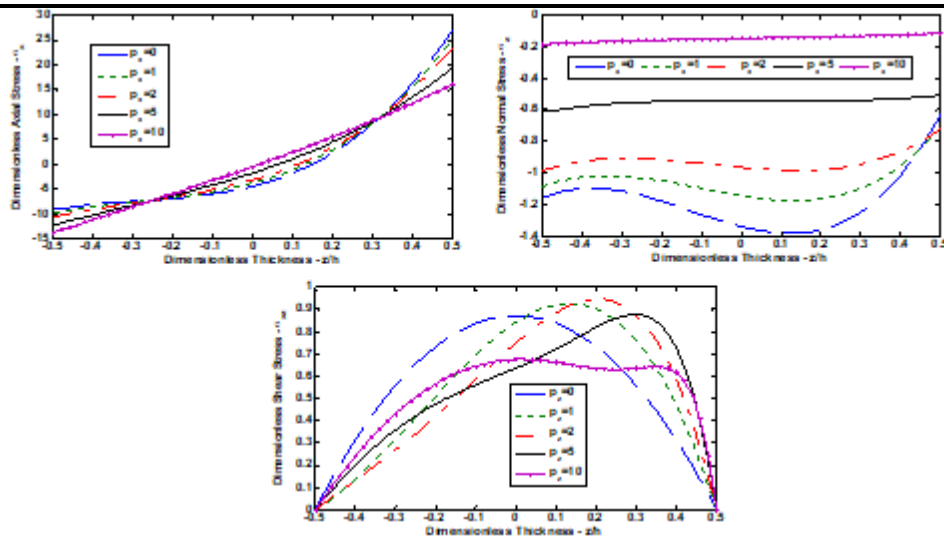
Figure 6. Dimensionless axial $\bar{\sigma}_x(\frac{L}{2}, z)$, normal $\bar{\sigma}_z(\frac{L}{2}, z)$ and shear stress $\bar{\sigma}_{xz}(0, z)$ through the thickness of the SS FGB for $p_z=2$ and $p_x=2$, L/h=20
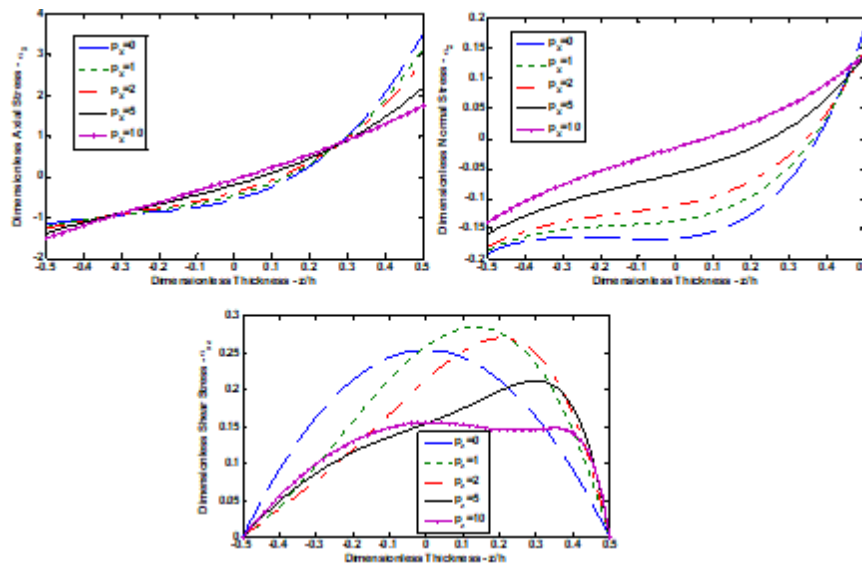
Figure 7. Dimensionless axial $\bar{\sigma}_x(\frac{L}{2}, z)$, normal $\bar{\sigma}_z(\frac{L}{2}, z)$ and shear stress $\bar{\sigma}_{xz}(0, z)$ through the thickness of the CS FGB for $p_z=2$ and $p_x=2$, L/h=5
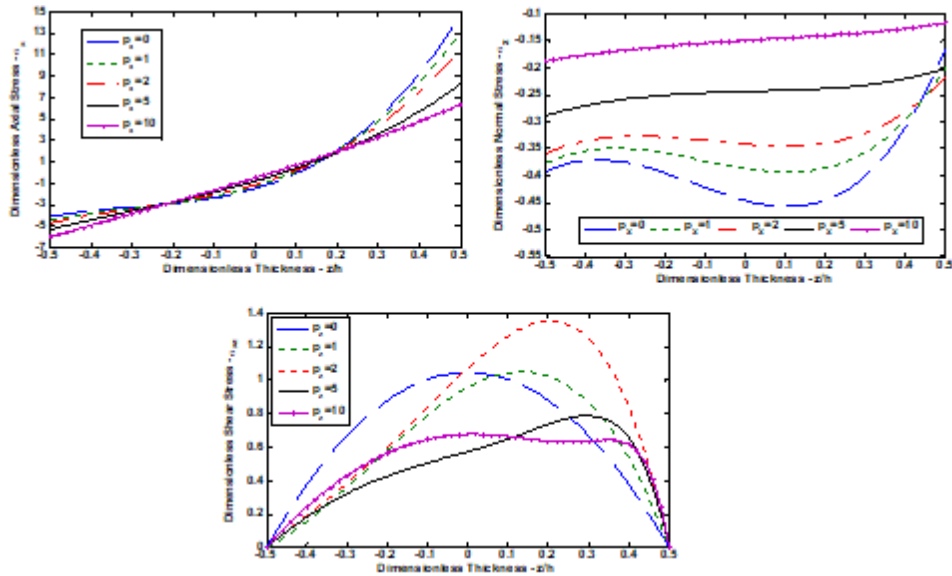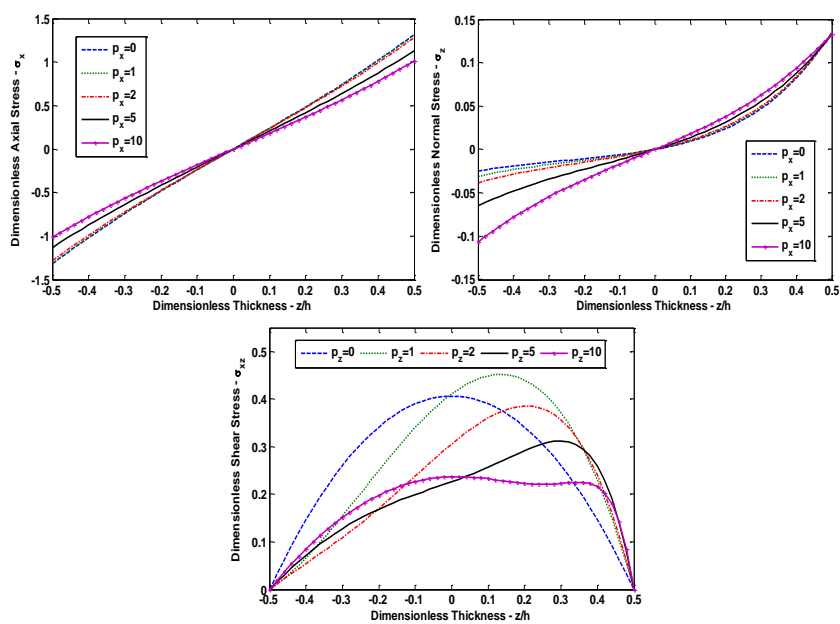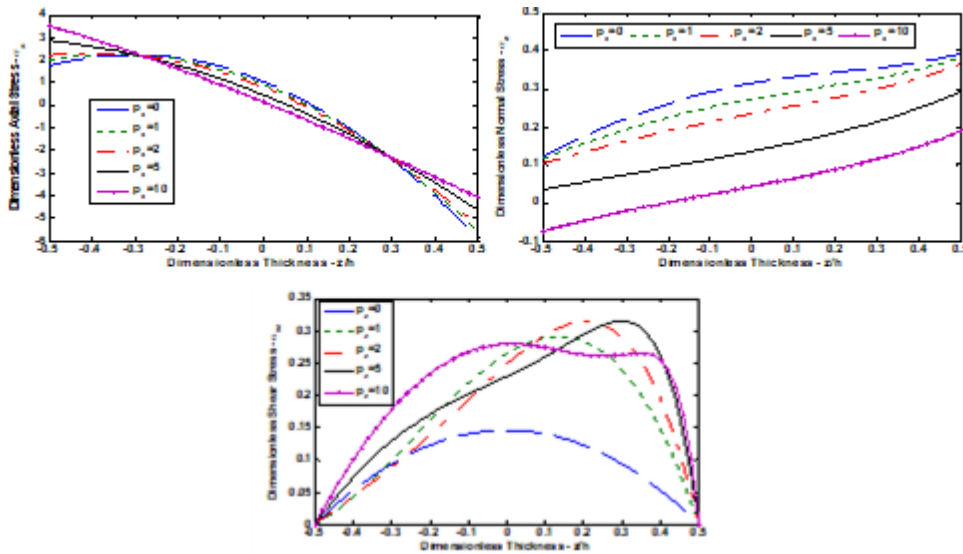
Figure 8. Dimensionless axial $\bar{\sigma}_x(\frac{L}{2}, z)$, normal $\bar{\sigma}_z(\frac{L}{2}, z)$ and shear stress $\bar{\sigma}_{xz}(0, z)$ through the thickness of the CS FGB for p_z=2 and p_x=2, L/h=20

Table 11. Dimensionless maximum transverse deflections of the C-C two-directional FGB for various gradation exponents in both directions.

Aspect Ratio (L/h)	p_z	Vo et al. [17]	p_x				
		$p_x = 0$	0	1	2	5	10
5	0	0.8327	0.8349	1.0660	1.3187	2.0188	2.6766
	1	1.5722	1.5868	1.8836	2.1655	2.8106	3.3063
	2	2.0489	2.0810	2.3585	2.6100	3.1762	3.5770
	5	2.6929	2.7180	2.9393	3.1597	3.5873	3.8630
	10	3.1058	3.1104	3.3217	3.4988	3.8290	4.0292
20	0	0.5894	0.5898	0.7532	0.9315	1.4187	1.8575
	1	1.1613	1.1630	1.3754	1.5737	2.0112	2.3388
	2	1.4811	1.4906	1.6764	1.8510	2.2307	2.5065
	5	1.7731	1.7762	1.9474	2.1065	2.4409	2.6534
	10	1.9694	1.9734	2.1479	2.2997	2.5867	2.7617

Figure 9. Dimensionless axial $\bar{\sigma}_x(\frac{L}{2}, z)$, normal $\bar{\sigma}_z(\frac{L}{2}, z)$ and shear stress $\bar{\sigma}_{xz}(0, z)$ through the thickness of the CC FGB for

Figure 10. Dimensionless axial $\bar{\sigma}_x(\frac{L}{2}, z)$, normal $\bar{\sigma}_z(\frac{L}{2}, z)$ and shear stress $\bar{\sigma}_{xz}(0, z)$ through the thickness of the CF FGB for p_z=1 and p_x=2, L/h=5

Table 12. Dimensionless maximum transverse deflections of the C-F two-directional FGB for various gradation exponents in both directions.

Aspect Ratio (L/h)	p_z	Li et al. [16] $p_x = 0$, $\varepsilon_z = 0$	Vo et al. [17] $p_x = 0$, $\varepsilon_z \neq 0$	p_x				
				0	1	2	5	10
2	0	38.4079		35.2697	38.8074	43.3814	58.5072	83.8566
	1	73.6361		67.7056	72.5379	78.1133	94.2687	116.6278
	2	96.4165	-	87.2699	91.4037	96.5571	109.5350	128.8880
	5	124.3960		109.6762	113.0652	116.5574	126.9298	141.5556
	10	143.2723		124.4861	127.9787	135.0984	137.1212	151.2053
3	0	32.4211		30.8511	33.7188	37.1688	49.7066	70.9790
	1	63.5249		59.6712	63.7506	68.1217	81.3383	100.2031
	2	82.3200	-	75.7549	80.0420	84.1371	96.7912	111.4601
	5	101.9579		92.9652	96.3159	100.7895	107.7395	122.6167
	10	114.9451		105.4147	109.0172	112.5187	119.6471	131.2405
5	0	29.3558	28.5524	27.6636	30.4944	33.6062	44.5715	63.7455
	1	58.3481	56.2002	56.7975	60.2980	64.0033	75.5193	93.3406
	2	75.1027	71.7295	71.6238	75.2135	78.7156	88.8993	103.9447
	5	90.4697	86.1201	86.5866	89.8121	92.9513	102.7237	114.2047
	10	100.3961	95.7582	97.6667	101.0233	104.1912	113.5742	123.2930

It is observed in Fig. 10 that the dimensionless axial stress values computed by using the shear and normal deformation theory formulation increases as the gradation exponent in the x direction decreases. It is clear that the maximum normal stress values are found at the top surface of the beam. As the gradation exponent in the x direction decreases, the maximum normal stress increases. The dimensionless shear stress values are shown in Fig. 10. As it is seen, the minimum shear stress value is obtained when the gradation exponent in the z direction is set to zero. The shear stress values are zero at the bottom and top surfaces of the beam.

6. CONCLUSION

The SSPH basis functions are employed to analyze the elastostatic behaviour of the two directional functionally graded beams subjected to different sets of boundary conditions and uniformly distributed load by using strong formulation of the problem. A shear and normal deformation theory which includes both shear deformation and thickness stretching effect is used to evaluate the transverse deflections, axial, normal and shear stresses of two directional FGBs. The developed code is verified by studying a simply supported FGB problem and comparing the results with previous studies and the analytical solutions. Four different boundary conditions (SS, CS, CC and CF) are considered with different gradation exponents in both directions and

various aspect ratios. The effect of the normal strain is investigated and it is found that it is important and should be considered in the static behavior of the two directional functionally graded beams including sandwich structures which may be a subject of the future studies.

Another important point is that for CF beam, the computed results for the aspect ratio which is higher than 5 are not agree very well with the previous studies as the gradation exponent in the x direction is set to higher than 2. At least within the scope of this work, it may be told that by using the SSPH method and present shear and normal deformation theory, it is not recommended to use a gradation exponent in the x direction greater than 2 as the aspect ratio increases with CF boundary condition and this should be investigated in future studies.

It is found that the SSPH method provides satisfactory results at least for the problems studied here. Based on the results of the four numerical examples, it is recommended that the SSPH method can be applied for solving linear two directional functionally graded beam problems by employing different shear deformation theories including shear and normal deformation theories.

REFERENCES

[1] Kadoli R., Akhtar K., Ganesan N., "Static analysis of functionally graded beams using higher order shear deformation theory", *Appl Math Model*, 32:2509-2525, (2008).

[2] Li X.F., "A unified approach for analyzing static and dynamic behaviors of functionally graded Timoshenko and Euler–Bernoulli beams", *Journal of Sound and Vibration*, 318:1210-1229, (2008).

[3] Menaa R., Tounsi A., Mouaici F., Mechab I., Zidi M., Bedia E.A.A., "Analytical solutions for static shear correction factor of functionally graded rectangular beams", *Mechanics of Advanced Materials and Structures*, 19:641-652, (2012).

[4] Li S.R., Cao D.F., Wan Z.Q., "Bending solutions of FGM Timoshenko beams from those of the homogenous Euler–Bernoulli beams", *Appl Math Model*, 37:7077-7085, (2013).

[5] Jing L.L., Ming P.J., Zhang W.P., Fu L.R., Cao Y.P., "Static and free vibration analysis of functionally graded beams by combination Timoshenko theory and finite volume method", *Compos Struct*, 138:192-213, (2016).

[6] Aydogdu M., Taskin V., "Free vibration analysis of functionally graded beams with simply supported edges", *Materials&Design*, 28:1651–1656, (2007).

[7] Simsek M., "Fundamental frequency analysis of functionally graded beams by using different higher-order beam theories", *Nuc Eng and Des*, 240:697–705, (2010).

[8] Simsek M., "Vibration analysis of a functionally graded beam under a moving mass by using different beam theories", *Compos Struct*, 92:904–17, (2010).

[9] Pradhan K.K., Chakraverty S., "Free vibration of Euler and Timoshenko functionally graded beams by Rayleigh-Ritz method", *Compos Part B*, 51:175–184, (2013).

[10] Su H., Banerjee J.R., Cheung C.W., "Dynamic stiffness formulation and free vibration analysis of functionally graded beams", *Compos Struct*, 106:854–862, (2013).

[11] Li S.R., Wan Z.G., Zhang J.H., "Free vibration of functionally graded beams based on both classical and first-order shear deformation beam theories", *Applied Mathematics and Mechanics*, 35:591–606, (2014).

[12] Aydogdu M., "Thermal buckling analysis of cross-ply laminated composite beams with general boundary conditions", *Composite Science and Technology*, 67:1096–1104, (2007).

[13] Akgöz B., Civalek Ö., "Buckling analysis of functionally graded microbeams based on the strain gradient theory", *Acta Mechanica*, 224:2185–2201, (2013).

[14] Aydogdu M., "Semi-inverse method for vibration and buckling of axially functionally graded beams", *Journal of Reinforced Plastics&Composites*, 27:683–91, (2008).

[15] Huang Y., Li X.F., "Buckling analysis of nonuniform and axially graded columns with varying flexural rigidity", *Journal of Engineering Mechanics*, 137(1):73–81, (2011).

[16] Li X.F., Wang B.L., Han J.C., "A higher-order theory for static and dynamic analyses of functionally graded beams", *Archieve of Applied Mechanics*, 80:1197-1212, (2010).

[17] Vo T.P., Thai H.T., Nguyen T.K., Inam F., Lee J., "Static behaviour of functionally graded sandwich beams using a quasi-3D theory", *Compos Part B*, 68:59-74, (2015).

[18] Filippi M., Carrera E., Zenkour A.M., "Static analyses of FGM beams by various theories and finite elements", *Compos Part B*, 72:1-9, (2015).

[19] Mashat D.S., Carrera E., Zenkour A.M., Khateeb S.A.A., Filippi M., "Free vibration of FGM layered beams by various theories and finite elements", *Compos Part B*, 59:269–278, (2014).

[20] Vo T.P., Thai H.T., Nguyen T.K., Inam F., Lee J., "A quasi-3D theory for vibration and buckling of functionally graded sandwich beams", *Compos Struct*, 119:1–12, (2015).

[21] Mantari J.L., Yarasca J., "A simple and accurate generalized shear deformation theory for beams", *Compos Struct*, 134:593–601, (2015).

[22] Mantari J.L., "A refined theory with stretching effect for the dynamics analysis of advanced composites on elastic foundation", *Mech Mater*, 86:31–43, (2015).

[23] Mantari J.L., "Refined and generalized hybrid type quasi-3D shear deformation theory for the bending analysis of functionally graded shells", *Compos Part B*, 83:142–152, (2015).

[24] Nguyen T.K., Vo T.P., Nguyen B.D., Lee J., "An analytical solution for buckling and vibration analysis of functionally graded sandwich beams using a quasi-3D shear deformation theory", *Compos Struct*, 156:238-252, (2016).

[25] Nemat-Alla M., "Reduction of thermal stresses by developing two-dimensional functionally graded materials", *Int Journal of Solids and Structures*, 40:7339–56, (2003).

[26] Goupee A.J., Vel S.S., "Optimization of natural frequencies of bidirectional functionally graded beams", *Struct Multidisc Optim*, 32:473–84, (2006).

[27] Lü C.F., Chen W.Q., Xu R.Q., Lim C.W., "Semi-analytical elasticity solutions for bidirectional functionally graded beams", *Int Journal of Solids and Structures*, 45:258–275, (2008).

[28] Zhao L., Chen W.Q., Lü C.F., "Symplectic elasticity for two-directional functionally graded materials" ***Mech Mater***, 54:32–42, (2012).

[29] Simsek M., "Buckling of Timoshenko beams composed of two-dimensional functionally graded material (2D-FGM) having different boundary conditions", ***Compos Struct***, 149:304–314, (2016).

[30] Karamanli A., "Elastostatic analysis of two-directional functionally graded beams using various beam theories and Symmetric Smoothed Particle Hydrodynamics method", ***Compos Struct***, 160:653-669, (2017).

[31] Karamanli A., "Bending behaviour of two directional functionally graded sandwich beams by using a quasi-3d shear deformation theory", ***Compos Struct***, 174:70-86, (2017).

[32] Donning B.M., Liu W.K., "Meshless methods for shear-deformable beams and plates", ***Comp Meth in Appl Mech and Eng***, 152:47-71, (1998).

[33] Gu Y.T., Liu G.R., "A local point interpolation method for static and dynamic analysis of thin beams", ***Comp Meth in Appl Mech and Eng***, 190(42):5515-5528, (2001).

[34] Ferreira A.J.M., Roque C.M.C., Martins P.A.L.S., "Radial basis functions and higher-order shear deformation theories in the analysis of laminated composite beams and plates", ***Compos Struct***, 66:287-293, (2004).

[35] Ferreira A.J.M., Fasshauer G.E., "Computation of natural frequencies of shear deformable beams and plates by an RBF-pseudospectral method", ***Comp Meth in Appl Mech and Eng***, 196:134-146, (2006).

[36] Moosavi M.R., Delfanian F., Khelil A., "The orthogonal meshless finite volume method for solving Euler–Bernoulli beam and thin plate problems", ***Thin Walled Structures***, 49:923-932, (2011).

[37] Wu C.P., Yang S.W., Wang Y.M., Hu H.T., "A meshless collocation method for the plane problems of functionally graded material beams and plates using the DRK interpolation", ***Mechanics Research Communications***, 38:471-476, (2011).

[38] Roque C.M.C., Figaldo D.S., Ferreira A.J.M., Reddy J.N., "A study of a microstructure-dependent composite laminated Timoshenko beam using a modified couple stress theory and a meshless method", ***Compos Struct***, 96:532-537, (2013).

[39] Qian L.F., Batra R.C., "Design of bidirectional functionally graded plate for optimal natural frequencies", ***Journal of Sound and Vibration***, 280:415-424, (2005).

[40] Pilafkan R., Folkow P.D., Darvizeh M., Darvizeh A., "Three dimensional frequency analysis of bidirectional functionally graded thick cylindrical shells using a radial point interpolation method (RPIM)", ***European Journal of Mechanics A/Solids***, 39:26-34, (2013).

[41] Yang Y., Kou K.P., Lu V.P., Lam C.C., Zhang C.H., "Free vibration analysis of two-dimensional functionally graded structures by a meshfree boundary–domain integral equation method", ***Compos Struct***, 110:342-353, (2014).

[42] Zhang G.M., Batra R.C., "Symmetric smoothed particle hydrodynamics (SSPH) method and its application to elastic problems", ***Comp Mech***, 43:321-340, (2009).

[43] Batra R.C., Zhang G.M., "SSPH basis functions for meshless methods, and comparison of solutions with strong and weak formulations", ***Comp Mech***, 41:527-545, (2008).

[44] Tsai C.L., Guan Y.L., Batra R.C., Ohanehi D.C., Dillard J.G., Nicoli E., Dillard D.A,. "Comparison of the performance of SSPH and MLS basis functions for two-dimensional linear elastostatics problems including quasistatic crack propagation", ***Comp Mech***, 51:19-34, (2013).

[45] Tsai C.L., Guan Y.L., Ohanehi D.C., Dillard J.G., Dillard D.A., Batra R.C., "Analysis of cohesive failure in adhesively bonded joints with the SSPH meshless method", ***Int Journal of Adhesion & Adhesives***, 51:67-80, (2014).

[46] Wong S.M., Hon Y.C., Golberg M.A., "Compactly supported radial basis functions for shallow water equations", ***Applied Mathematics and Computation***, 127:79-101, (2002).